BIOCHEMISTRY

 Volume 43, Number 14 April 13, 2004

Current Topics

Structural Dynamics and Processing of Nucleic Acids Revealed by Single-Molecule Spectroscopy†

Taekjip Ha*

Department of Physics and Center for Biophysics and Computational Biology, University of Illinois, Urbana-Champaign, Urbana, Illinois 61801 USA

Received January 2, 2004; Revised Manuscript Received March 2, 2004

ABSTRACT: Single-molecule fluorescence spectroscopy is a powerful method to observe real time movements of individual biological molecules while they are functioning without the need for synchronization. Dynamic characteristics of nucleic acids can now be easily and reliably studied, and new applications are emerging in which their recognition and processing by proteins and enzymes are being understood with unprecedented detail. The most recent examples are discussed, including the hairpin ribozyme, Holliday junction, G-quadruplex, Rep helicase, reverse transcriptase, and combination with mechanical manipulation.

Nucleic acids play essential roles in the cellular cycle. Their structures are recognized and handled by many nucleic acid binding proteins and enzymes. Ideally, one would like to measure static structures and dynamic properties of nucleic acids and understand how these structural properties influence the activities of proteins that act on them. In the case of ribozymes, the processing power is built into the molecules themselves, and because of the relative simplicity, intricate coupling between the structure and function can be studied with greater control than for protein enzymes.

Recently developed fluorescence assays allow the real time detection of biochemical reactions and accompanying conformational changes. However, it is often difficult to distinguish signal contributions by the functional and structural dynamics. For example, an apparent cleavage rate of a ribozyme may be a combination of the actual chemical reaction as well as structural dynamics such as RNA folding, unfolding, and product release. There are also examples in which reactions or structural changes cannot be synchronized, precluding the use of conventional kinetic tools such as stopped-flow fluorescence. In such problems, single-molecule fluorescence techniques offer unique capabilities to dissect their molecular mechanisms in greater detail (*1*, *2*). Although several other single-molecule approaches exist utilizing aspects such as localization (*3*), fluorescence polarization (*4*), lifetimes (*5*), and quenching (*6*), the most popular, and arguably most general, is the technique of fluorescence resonance energy transfer (FRET).

In a typical FRET experiment (*7*, *8*), a biological macromolecule is labeled with a donor fluorophore and an acceptor fluorophore at two different positions. The internal motion of the molecule can bring the two fluorophores closer to or farther from each other, resulting in distance changes. FRET efficiency *E*, defined as the fraction of donor excitation events that result in the excitation of the acceptor, is a strong

† Funding during the preparation of this manuscript was provided by the National Institutes of Health and the National Science Foundation.

* To whom correspondence should be addressed. E-mail: tjha@uiuc.edu.

10.1021/bi049973s CCC: $27.50
Published on Web 03/17/2004

function of the distance R between the two molecules, according to

$$E = \frac{1}{1 + \left(\frac{R}{R_0}\right)^6}$$

Here R_0 is the distance at which E is 50% and is typically in the range of 3−7 nm, an ideal length scale for many macromolecules. Hence, FRET measured at the single molecule level can report on the conformational changes of biological molecules in real time that are often difficult to observe in conventional ensemble studies (*9*). The power of single-molecule FRET in biophysical applications has been well-established. Starting from the proof of principle experiments in which FRET between a single pair of donor and acceptor molecules was reported (*10*), the field went through a validation process of showing that the technique indeed works (*11*−*14*), into the discovery period where new and interesting information is being uncovered using the technique (*15*−*34*). Single-molecule FRET methodology has been reviewed elsewhere (*9*, *35*). In this review, I will discuss some of the most recent developments concerning RNA, DNA, and proteins that interact with DNA, and future technical challenges, but it is important to mention in passing that similar approaches have been used for protein folding, protein conformational changes, and protein−protein interactions.

RNA: HAIRPIN RIBOZYME

Ribozyme Folding and Catalysis. Folding is a process in which a macromolecule obtains the proper three-dimensional structure necessary for functioning. The final form is determined by the linear sequence of the polymer itself, and hence folding is spontaneously driven, in most cases, given the right conditions. In an ideal folding study, the folding trajectory would be measured and analyzed, but also the folded molecule would be shown to be active biologically. This is not always an easy task for proteins, but there have been several single-molecule experiments in which this has been tested for ribozymes (*15*, *18*, *36*). Figure 1 shows an example of the hairpin ribozyme folding and cleavage reaction (*18*).

The natural form of the hairpin ribozyme comprises two major structural elements; a four-way RNA junction and two internal loops carried by adjacent A and B arms of the junction (Figure 1a). Mg^{2+} ions promote folding via the docking of the two loops, and cleavage and ligation reactions of a specific bond occur within the active site. Fluorescent labeling of the ends of A and B arms with the donor and acceptor allows the monitoring the ribozyme folding that brings the fluorophores in close proximity, yielding high FRET. Figure 1b shows a time record of the fluorescence intensities of the donor and acceptor from a single ribozyme immobilized to a glass surface via biotin−streptavidin linker. It started from the unfolded low FRET state (high donor signal and low acceptor signal) in the absence of Mg^{2+}. At time $t = 35$ s, a buffer containing 10 mM Mg^{2+} was flowed into the sample, and the molecule folded immediately as marked by an abrupt increase in FRET (donor signal decrease and acceptor signal increase). The molecule remained stably folded until 180 s when it started showing rapid fluctuations

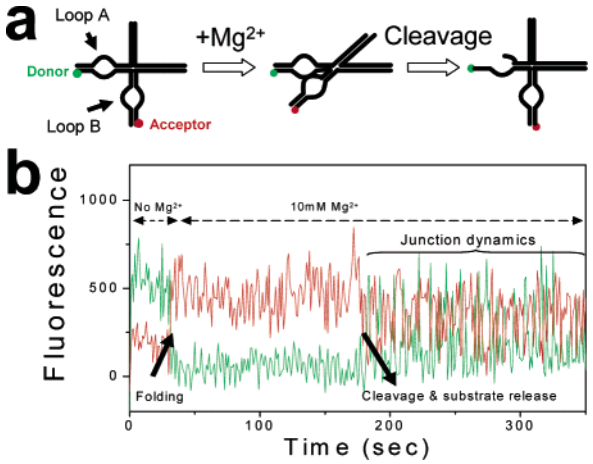

FIGURE 1: Hairpin ribozyme folding and cleavage. (a) A simplified scheme for detecting folding and catalysis of the hairpin ribozyme via FRET between the donor and acceptor fluorophores attached to the two helices carrying the essential loops A and B. (b) An example time record of donor (green) and acceptor (red) fluorescence intensities as a hairpin ribozyme folds (donor signal goes down and acceptor signal goes up due to FRET increase upon ribozyme folding at 35 s when Mg^{2+} is added), and cleavage and product release occur (∼180 s) after which the four-way junction dynamics show anticorrelated signal fluctuations of the donor and acceptor. Adapted from ref *18*.

due to the intrinsic dynamics of the junction (*25*), indicating that the cleavage product had been released. Comparisons to bulk solution cleavage experiments showed that the overall reaction rate was not perturbed by dye labeling or surface immobilization (*18*).

Ribozyme Folding: Persistent Heterogeneity. One of the most fascinating discoveries afforded by single-molecule spectroscopy of biomolecules is the molecular heterogeneity. This was first reported for cholesterol oxidase by Xie and colleagues (*37*). The first hint of heterogeneity in single-molecule RNA studies came from the studies of an RNA three-way junction (*14*). Since the folding and unfolding rates were faster than the time resolution, only the time averaged values were measured, and these values showed much broader distribution than was expected from statistical noise alone, leading to the suggestion that there is a distribution of the free energy difference between the folded and unfolded states. Perhaps the most spectacular example was found in the hairpin ribozyme. The minimal form, i.e., that lacks the junction, was shown to have a single rate of folding but four different rates of unfolding that cover 3 orders of magnitude in range (*36*). The natural form was also highly heterogeneous showing widely different rates not only for unfolding but also for folding (*18*). Figure 2a shows two FRET efficiency traces of individual hairpin ribozyme molecules in 0.5 mM Mg^{2+}. They show markedly different folding kinetics even though they are nominally identical and observed under the same conditions. These heterogeneities are remarkable in that they are very persistent. Each molecule appears to have its own clock and fluctuates for minutes or longer at the same rates even though there is a huge variation in the rates between molecules. RNA is a complex molecule, and it is not too difficult to imagine that such heterogeneities may arise from slight differences in the substructures (*36*). Yet considering that the loop−loop interface undergoes major structural changes upon docking, how the substructures can

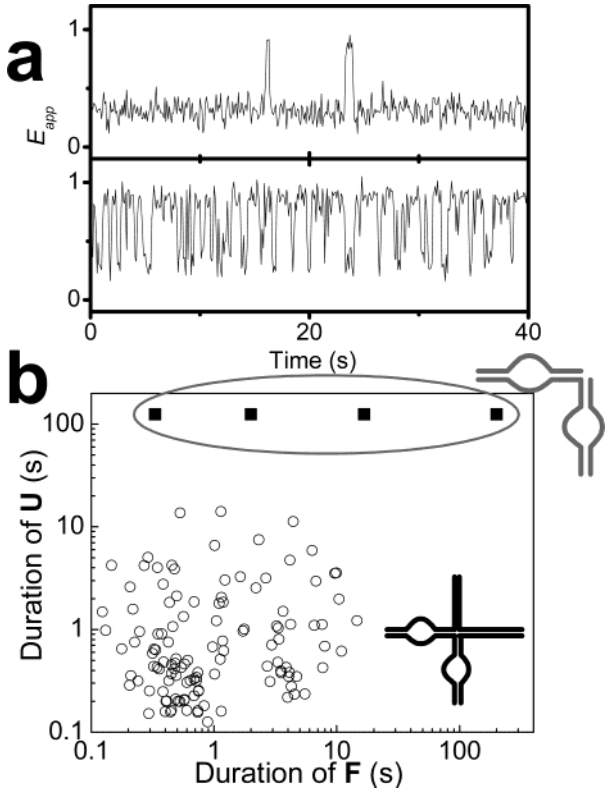

FIGURE 2: Persistent heterogeneity in hairpin ribozyme folding kinetics. (a) Example time records of apparent FRET efficiency $E_{app} \equiv 1/(1 + I_D/I_A)$, where I_D and I_A are fluorescence intensities of donor and acceptor attached to the hairpin ribozyme as shown in Figure 1. High FRET state and low FRET state correspond to the folded and unfolded state, respectively. These two nominally identical molecules show similar duration of the folded state but markedly different durations of the unfolded states even under the same conditions (0.5 mM Mg^{2+}). (b) Average duration of the folded (F) and unfolded (U) states of 125 hairpin ribozyme molecules in 0.5 mM Mg^{2+} in log−log scale (open circles). Also shown are four distinct lifetimes of the folded state observed from the minimal form of the hairpin ribozyme (filled square). Adapted from refs *18* and *36*.

persist over multiple folding and unfolding events is a mystery.

Can this molecular heterogeneity be an experimental artifact? Different molecules may interact with the surface environment differently, altering their kinetics. In addition, the heterogeneity may arise from real chemical differences, for instance, due to possible imperfections in the chemical synthesis of oligonucleotides. These possibilities are extremely difficult to rule out. Zhuang et al. earlier reported highly heterogeneous unfolding rates (but homogeneous docking rate; see Figure 2b, filled symbols) in the case of the minimal form of the hairpin ribozyme and argued that such heterogeneity can quantitatively explain complex reaction kinetics measured in bulk solution (*36*). But their analysis made several assumptions that were not independently verified (for instance, it was assumed that different species of markedly different stabilities of the folded state share a single cleavage rate and a single ligation rate, and that the folding and unfolding rates measured from the mutated, noncleavable, or nonligatable ribozymes are identical to those of functional ribozymes) and was not meant to be a definite proof that there was no surface effect. Tan et al observed the same degree of heterogeneity using two

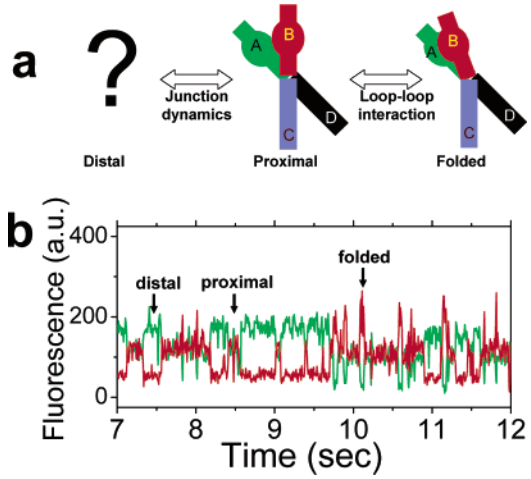

FIGURE 3: Hairpin ribozyme is a three-state folder. (a) Proposed model for the stepwise folding of the hairpin ribozyme. The ribozyme undergoes folding into the active conformation in two stages, corresponding to the properties of the junction, and the interactions between the loops. The structural dynamics of the junction promotes rapid active site formation due to the spontaneous fluctuations between the two states of the junction, distal and proximal. The distal state comprises a number of distinct conformations that cannot be distinguished on the basis of our current data. (b) Single-molecule FRET time record of a C25U variant hairpin ribozyme fluctuating between the distal, proximal, and folded states. Donor intensity in green and acceptor intensity in red. Adapted from ref *18*.

different surfaces, BSA coated and PEG coated, but it hardly constituted a proof that the surface did not contribute to the observed heterogeneity (*18*). Clearly, new kinds of experiments are needed to unambiguously test whether the heterogeneity is real and intrinsic, and if so what the physical mechanism is, and whether there is any functional significance or it is simply an accident tolerated by nature.

Ribozyme Folding: Speed Limit. The folding of RNA appears to be relatively slow. The minimal form of the hairpin ribozyme takes more than 100 s to fold even in 12 mM Mg^{2+} (Figure 2b). The presence of the junction in the natural form enhances the folding substantially, with typical folding rates higher than 1 s^{-1} even at 0.5 mM Mg^{2+} (Figure 2b). Is such an enhancement necessary, while clearly adequate, for the ribozyme's function in vivo? How does the four-way junction enhance the folding to such a degree?

Tan et al reported that the unfolded hairpin ribozyme does not have a single conformation but rather consists of at least two states that are termed proximal and distal states (*18*). These two states are derived from the junction because similar two-state fluctuations were observed from an RNA four-way junction where the loops were replaced by complete Watson−Crick base pairing. The proximal state brings the two loops in close proximity, increasing the probability of interaction between them and thus folding (Figure 3a). The most direct evidence for this mechanism of folding enhancement came from studies of a hairpin ribozyme variant (C25U) with disrupted folding so that all three states (distal, proximal, and folded) are populated similarly. Figure 3b shows that a C25U molecule fluctuates among three FRET states and that a trip to and from the folded high FRET state always entails a stopover at the proximal intermediate FRET state.

Folding occurs on the 100 ms time scale for the natural form in physiologically relevant solution conditions (Figure

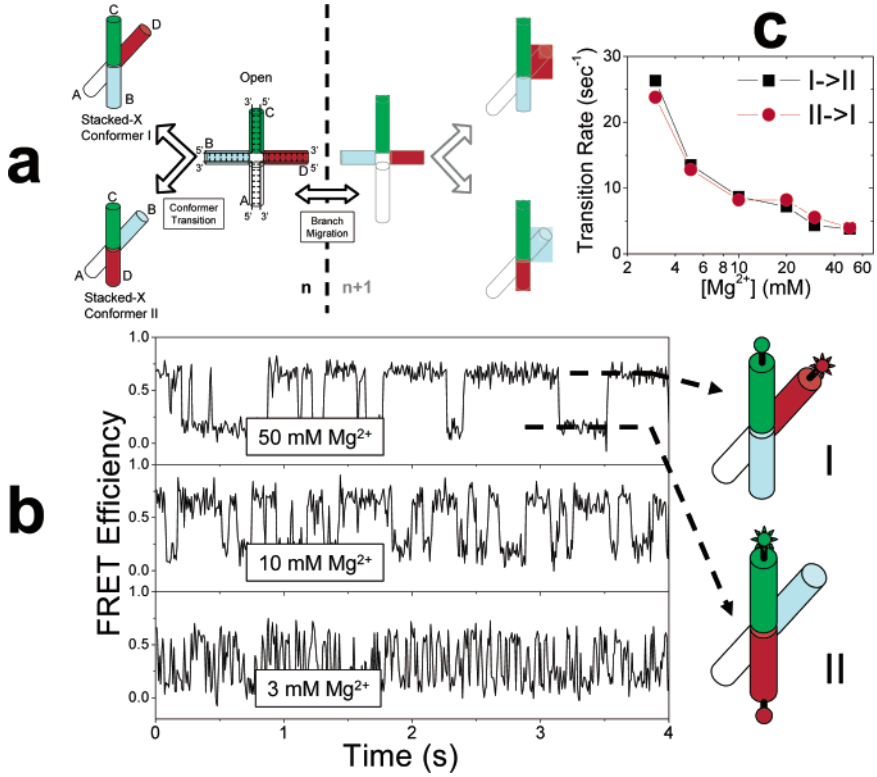

FIGURE 4: Structural dynamics of single Holliday junctions. (a) Cartoons illustrating the structures of Holliday junction. The "open structure" shows four single-stranded DNA meeting to form a junction of four helices (A, B, C, and D). With Mg^{2+}, two neighboring helices can stack against each other to form a "stacked-X structure". Two stacking conformers are possible, depending on the stacking partners. The open structure is considered a common intermediate for transitions between conformers and branch migration. (b) Single-molecule FRET time records of Holliday junctions at three different Mg^{2+} concentrations. Donor and acceptor dyes are attached to give higher FRET for conformer I than for conformer II. (c) Conformer transition rates as a function of Mg^{2+} concentration. Both forward and backward rates decrease with increasing Mg^{2+} concentration while remaining close to each other. Adapted from ref *17*.

2b). Since the junction dynamics is substantially faster, many attempts (visits to the proximal intermediate state) are needed for folding. Why does the folding not occur even faster? It is possible such folding rates are adequate for biological functions of the ribozyme, and there may have been no evolutionary pressure to improve upon it. Still one can ask what physically limits the folding rate.

To probe what limits the speed of ribozyme folding in general, careful single-molecule studies of the folding transition state have been made for the *Tetrahymena* ribozyme (*23*) and the minimal form of the hairpin ribozyme (*22*). The rates of folding and unfolding were measured as a function of mutations designed to disrupt specific interactions found in the folded form. If the mutation alters the folding rate, but not the unfolding rate, one can conclude that the transition state is more similar to the folded state than to the unfolded state insofar as that particular interaction is concerned. In contrast, all of the single-molecule analyses have shown that mutations alter the unfolding rate much more than the folding rate, suggesting that most of the native contacts are not yet formed in the transition state. By definition, once a molecule reaches the transition state it has equal probabilities to move toward the folded state and unfolded state. If the native contacts have not been formed in the transition state, what makes the transition state so capable of folding? Perhaps the folding is highly cooperative once the transition state brings the partners in close proximity with correct orientations.

DNA DYNAMICS: HOLLIDAY JUNCTIONS AND G-QUADRUPLEX

Unlike RNA, DNA is often thought of as a static (boring) molecule whose main role is in information storage. Two naturally occurring exceptions are DNA four-way junctions called Holliday junctions and G-quadruplexes.

Holliday Junction Conformational Dynamics. The Holliday junction is formed as a key intermediate in DNA recombination by combining two homologous DNA molecules (*38*). To understand how different enzymes recognize and process the Holliday junction during recombination, its intrinsic structural properties need to be known in detail. The Holliday junction can undergo two major structural dynamics, stacking conformer transitions and branch migration, which are strongly dependent on the types and concentrations of metal ions in solution. In the absence of divalent metal ions such as Mg^{2+}, the Holliday junction takes a so-called "open structure" where each of the four helices point to a corner of a square (Figure 4a) (*39*). In the presence of Mg^{2+}, a more compact structure called a "stacked-X structure" is formed (*40*, *41*). Neighboring helices are stacked against each other to form super-helices, and two super-helices subtend an acute angle between them, hence the name stacked-X structure (Figure 4a). By symmetry, there are two alternative stacking partners for each helix; hence, there should be two different conformations (conformer I with A stacked on D

and C stacked on B vs conformer II with A on B and C on D) (*42*, *43*).

McKinney et al. (*17*) attached fluorescent probes to the Holliday junction so that one conformer has higher FRET than the other and thus observed individual Holliday junctions fluctuating between the two stacking conformers (Figure 4b). Remarkably, the fluctuation rate decreased substantially with increasing Mg^{2+} concentration, but the relative populations remained constant (Figure 4b,c). This is in stark contrast to RNA folding where an increase in Mg^{2+} concentration increases the folded state population. Therefore, unlike in RNA folding, the rates of stacking conformer transitions cannot be measured using conventional stopped-flow techniques, making them truly nonsynchronizable dynamics.

Why does adding more Mg^{2+} slow the dynamics? The crystal structure of the Holliday junction shows four negatively charged phosphate groups at the exchange point within 6 Å of each other (*44*), leading to unfavorably strong electrostatic repulsion that can only be screened by metal ions. To change stacking partners, the helices have to be first unstacked from neighboring helices, which happens less frequently if the stacked structure is further stabilized by increasing Mg^{2+} concentration. Branch migration has also been shown to be slowed by 1000-fold upon Mg^{2+} addition (*45*), and it is likely that some sort of open structure is the common intermediate for branch migration and stacking conformer transitions (*17*).

Most structural studies of the Holliday junction used nonmigratable junctions where DNA sequences do not allow branch migration. Will the stacking conformer transitions occur in the context of a migratable junction? How are conformer transitions related to branch migration? How do the complex structural dynamics of the Holliday influence the activities of junction processing enzymes? Single-molecule fluorescence techniques appear to be well-poised to address these interesting questions.

G-Quadruplex. Eukaryotic chromosomes are terminated by telomeres whose primary function is to protect chromosomes from recombination and degradation. Disruption of telomere maintenance leads to eventual cell death, which can be exploited for therapeutic intervention in cancer. The DNA of human telomeres consists of repeats of the nucleotide sequence TTAGGG, ending in a single-stranded segment that overhangs at the end of the double-stranded DNA helix.

High-resolution structural studies of the human telomeric sequence (*46*, *47*) revealed G-quadruplex formation where four guanines are hydrogen bonded with each other in a horizontal planar arrangement and three such layers are stacked on top of each other (Figure 5a). Two significantly different topologies have been observed with respect to the orientation of the four strands. In an earlier NMR study in Na^+ solution, an antiparallel structure (Figure 5a) was observed where two of the strands are running in opposite directions of the other two strands (*46*). In contrast, a recent X-ray structure obtained in K^+ solution showed a parallel structure (Figure 5a) where all four strands run in the same direction (*47*). Are different ions responsible for the two different structures? Or do both structures coexist and interconvert under any solution condition but did the crystallization process choose one over the other? Recent single-molecule FRET studies of G-quadruplex by Ying et al. (*24*) began to tackle these questions.

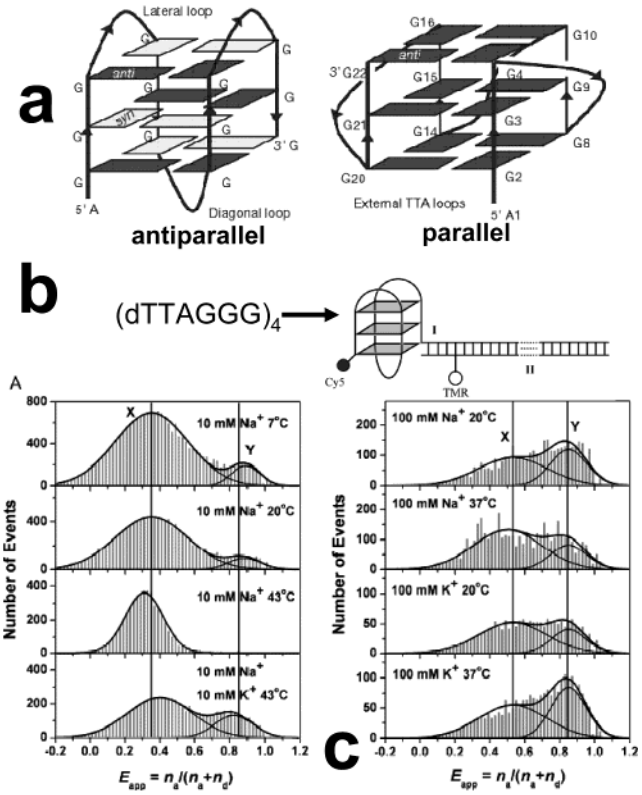

FIGURE 5: Multiple conformations of human telomeric DNA. (a) Parallel and antiparallel conformations of G-quadruplex. (b) Fluorescent DNA used for single-molecule FRET studies of G-quadruplex formed by human telomeric sequence. (c) FRET efficiency histograms obtained in various solutions containing Na^+ or K^+ as a function of temperature. Each histogram can be fit using two Gaussian peaks. Adapted from ref *24*.

As illustrated in Figure 5b, a partial duplex DNA with a single-stranded DNA overhang containing four repeats of the human telomeric sequence was fluorescently labeled so that FRET is high if a relatively compact structure such as G-quadruplex forms. Interestingly, two FRET peaks were observed from such a sample and their relative populations were dependent on ionic type and temperatures (Figure 5c). It is likely that these two FRET peaks are due to different conformations and the authors assigned them to the antiparallel (intermediate FRET) and parallel (high FRET) structures. Since it is not obvious a priori which structure would give smaller (or larger) separation between the dyes, molecular dynamics simulations were used to help the assignment. An independent experimental test of the assignment is not available yet.

Do these two conformations interconvert? If so, the conversion must be slower than 1 ms, the integration time used. The FRET measurements were performed while the molecules were diffusing in solution so any interconversion slower than 1 ms could not be observed. To switch between the parallel and antiparallel structures, the molecule must unfold to make a single-stranded form, and this form would also be necessary for hybridization to a complementary strand. Indeed, when a DNA complementary to the G-quadruplex forming sequence was added, the two FRET peaks disappeared in several minutes and a low FRET peak

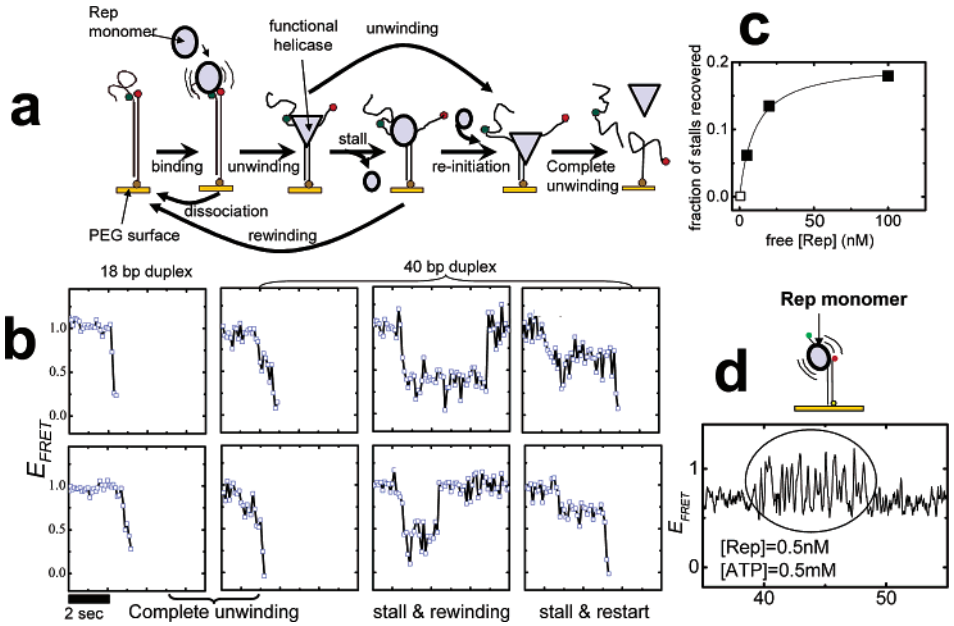

FIGURE 6: Helicase-catalyzed DNA unwinding. (a) Cartoons illustrating single-molecule unwinding experiments and proposed model for *E. coli* Rep helicase activity. Dye-labeled DNA is tethered to a PEG surface and the helicase interacts with DNA, changing DNA conformations. (b) Single-molecule FRET records of 18mer and 40mer duplex DNA unwinding. For 40mer unwinding, frequent stalls were observed that ended in DNA rewinding or unwinding restart. (c) Unwinding restart requires free helicase protein in solution because the fraction of unwinding stalls recovered is a strong function of protein concentration. (d) A burst of rapid conformational fluctuations is observed when a Rep helicase monomer binds to the DNA in the presence of DNA. These fluctuations are futile and do not lead to DNA unwinding. Adapted from ref *16*.

appeared, indicating duplex formation (*24*). Interconversion between parallel and antiparallel forms therefore must occur on a time scale between 1 ms and minutes, calling for single-molecule studies of immobilized molecules to determine their rates directly. Such dynamic characteristics of the G-quadruplex might be important in regulating the enzymatic access to the telomere and in providing recognizable features for telomere processing enzymes (*48*).

DNA PROCESSING ENZYMES AND DNA−PROTEIN INTERACTIONS

The next logical step in the studies of DNA metabolism is the inclusion of proteins that interact with DNA. The immediate challenge is much more severe surface interactions of proteins compared to nucleic acids, and this has been overcome by passivating the surface via polymer coating (*16*) or by studying the DNA−protein complexes diffusing in solution (*26*, *49*). Thus far, single-molecule FRET has been used for staphylococcal nuclease (*12*), *Escherichia coli* Rep helicase (*16*), HIV reverse transcriptase (*26*), and NgoMIV restriction endonucleases (*49*).

Helicases. Helicases couple conformational changes induced by ATP binding and hydrolysis to the unwinding of nucleic acids (*50*). They can also move along DNA track using ATP as fuel; hence, they are considered motor proteins. Recently, single-molecule techniques have been used to visualize the motion of a highly processive helicase, *E. coli* RecBCD, with up to 100 bp resolution (*51*, *52*). However, most helicases are not very processive in vitro, falling off DNA long before unwinding 100 bp. Ha et al. (*16*) developed a new single-molecule FRET-based helicase assay that can detect the DNA unwinding of less than 10 bp (Figure 6a), allowing them to detect, for the first time for any helicase, unwinding stalls, rewinding, and unwinding restart and to deduce their underlying mechanisms.

In this assay, the fluorescent probes are attached to the DNA where the unwinding begins. Therefore, FRET is almost 100% before unwinding and decreases as unwinding progresses, reporting on the extent of unwinding (Figure 6a,b). In the studies of the *E. coli* Rep helicase, the unwinding often stalled for a few seconds, either leading to DNA rewinding (FRET returns to 100%) or unwinding restart and completion (Figure 6b). The unwinding initiation required the action of more than a helicase monomer (*16*, *53*), and the unwinding restart required free helicase molecules in solution (Figure 6c). Therefore, it was proposed that the unwinding stalls when the active helicase complex dissociates, leaving a monomer on the DNA, and that the rewinding is observed if the remaining monomer dissociates. The unwinding can be restarted if additional helicase monomer(s) binds to the stalled monomer (Figure 6a). The helicase monomer was seen to undergo rapid ATP-dependent conformational fluctuations upon encountering the single-stranded/double-stranded DNA junction (Figure 6d), but these fluctuations are futile and do not lead to DNA unwinding.

Many outstanding questions about helicase mechanisms may be addressable using related approaches. Why do many helicase require oligomers (dimer, trimer, hexamer...) to function? How many base pairs are unwound per ATP hydrolyzed? What determines the directionality in DNA unwinding and translocation? How does the helicase couple conformational changes induced by ATP hydrolysis cycle to the unwinding action? Future experiments using fluorescently labeled helicases may detect the conformational changes of the enzyme and the DNA unwinding simultaneously, thereby directly probing the heart of the structure−function relationship.

Reverse Transcriptase. Crystal structures of DNA−protein complexes provide atomic details of the structural features

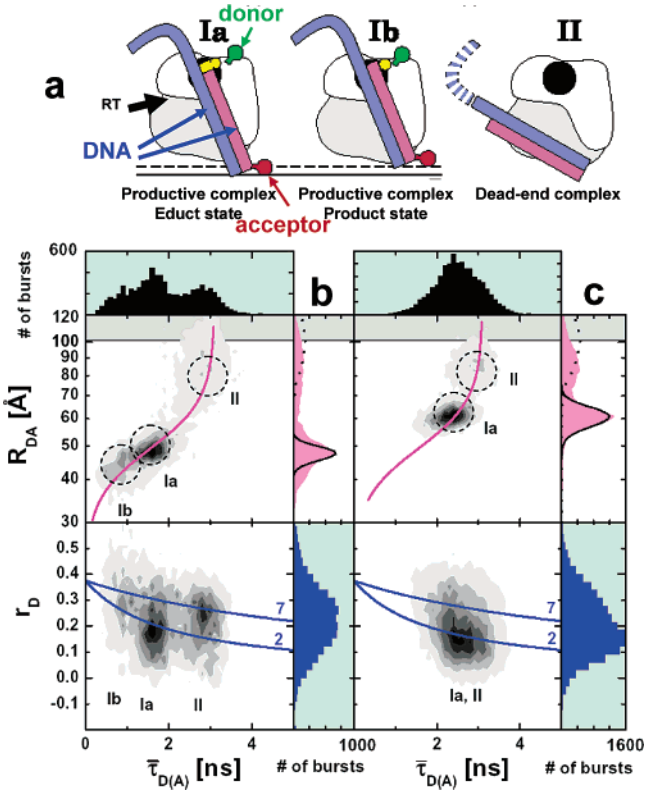

FIGURE 7: Structural heterogeneity of reverse transcriptase-DNA complexes (a) HIV-1 reverse transcriptase (RT) is labeled with a donor (Alexa488) and the DNA substrate has an acceptor (Cy5). On the basis of single-molecule experiments, it was proposed that the RT−DNA complex exists in three forms: two productive complexes that differ by 5 Å in donor−acceptor distances (I_a and I_b) and a dead end complex (II). (b) Two-dimensional density plots for distance vs donor lifetime and donor anisotropy vs donor lifetime. Proposed three populations (I_a, I_b, and II) are marked by dashed circles. (c) Same as in panel b, but after limited incorporation of nucleotides so that productive complexes now have larger distances. Adapted from ref *26*.

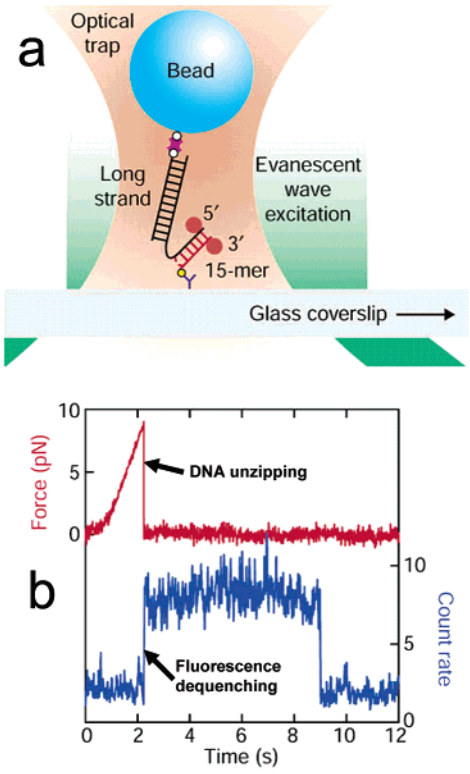

FIGURE 8: Combined force and fluorescence measurements of single DNA (a) A schematic diagram of an optical trap holding a bead which is connected to the surface via a fluorescently labeled DNA under investigation. Application of force between the two attachment points will unzip 15mer duplex DNA at the end of which are attached two rhodamine molecules. (b) Simultaneous recordings of force and fluorescence. As the surface is move relative to the trap, force increases until the DNA is unzipped and force returns to zero since the bead is not tethered to the surface anymore (red). Fluorescence of the rhodamine dyes is initially self-quenched due to proximity and increases abruptly upon DNA unzipping because the remaining single dye on the surface is no longer quenched by the other dye. At 9 s, the remaining dye photobleaches. Adapted from ref *58*.

that are important for their interactions and functions. However, it is very likely that there exist alternative structural organizations of these complexes that have not been crystallized. Furthermore, conditions used for crystallization often deviate from more physiologically relevant solution conditions and the crystal packing interactions may distort the structure. FRET can be useful in elucidating the global geometry of DNA−protein complex in physiological conditions. Single-molecule FRET can distinguish, with relative ease, labeling heterogeneities in fluorescently labeled proteins and hence obtain more quantitative information than ensemble FRET.

Rothwell et al. (*26*) made the first step in this direction by measuring FRET between a donor attached to a HIV-1 reverse transcriptase (RT) and an acceptor attached to a partial duplex DNA (Figure 7). In this tour de force experiment, not only were FRET efficiencies determined but also measured simultaneously were fluorescence lifetimes of the donor and acceptor dyes and their steady-state and time-resolved anisotropies. All these quantities were gleaned from single RT−DNA complexes within a few milliseconds while they are diffusing through a focused laser beam! Also developed were sophisticated analysis schemes that utilize all available information to deduce the distance distributions quantitatively and to discriminate against potential dye artifacts. These new techniques allowed them to distinguish three distinct RT−DNA complexes and to make their functional assignments (Figure 7).

FUTURE CHALLENGES

Thus far, single-molecule fluorescence studies have been limited to relatively simple and small systems consisting of a couple of interacting molecules. However, many biological macromolecules function in the context of larger macromolecular complexes, for instance, helicases as a part of chromatin remodeling enzymes or repliosome. An important step in the application of single-molecule fluorescence techniques is being made for the ribosome, the mother of all ribozymes (Steven Chu, private communication). These exciting and challenging tasks will require better tools, including robust immobilization techniques that maintain molecular functions and spectroscopic approaches to measure the coordinated movements of the system simultaneously. Below are two examples of very recent technical developments that are expected to make the single-molecule fluorescence studies more powerful and useful.

Combined Force and Fluorescence Measurements on Nucleic Acids. As has been discussed so far, single-molecule

fluorescence measurements can step-by-step piece together the motion of biomolecules. Yet, biomolecules in a cell perform their functions under a variety of environmental conditions, such as electrochemical potential for ion channels, and force and load for molecular motors. Hence, to understand their behavior, we must emulate these environmental variables. Techniques such as electrical patch clamping or optical trapping apply these forces, and are now well established. Yet, by themselves, they do not have the selectivity to isolate which parts of the biomolecule are undergoing shape changes responsible for the molecule's behavior. Combining fluorescence with manipulation makes this connection. Such a combination, while ambitious, is feasible: Yanagida and colleagues performed heroic experiments in which force and fluorescence measurements were combined in single molecules (*54*, *55*). However, the fluorescence measurements were limited to the binding and dissociation of fluorescent ATP analogues (*54*) and fluorescently labeled enzyme (*55*). More recently, a combination of FRET measurements and single channel recording was demonstrated for gramicidin (*56*, *57*). In these works, FRET was used to report on the assembly of gramicidin monomers to form the active dimeric species.

Another significant step was reported by the Block laboratory that combined optical tweezers with single-molecule fluorescence measurements (*58*). They measured the mechanical unzipping of duplex DNA via force and fluorescence dequenching, marking the first example of force-induced "structural change" of single molecules measured via fluorescence (Figure 8). Clearly, the same approach should work for single-molecule FRET, and it will be interesting to test how the folding properties of the hairpin ribozyme, for instance, are influenced by applied force. Folding and unfolding of simple RNA secondary structures have been measured as a function of applied force via mechanical measurements alone (*59*). However, the mechanical measurements do not allow the detection of conformational changes at low forces because of the flexibility of the long DNA tethers used. In contrast, FRET measurements can be performed at arbitrarily low forces (in fact, all the studies reviewed here were performed under zero applied force!).

Better Probes: Quantum Dots? An ideal fluorescent probe for single-molecule studies would possess as many as possible of the following characteristics. They have to be photostable, bright, bioconjugatable, small, and show little intensity fluctuations. Several popular dyes such as Cy3 and Cy5 as donor and acceptor in FRET studies generally satisfy these requirements for many applications. However, improvement on their properties is still desirable so that faster and smaller movements can be detected for a longer time. In addition, it has yet to be shown that conformational dynamics of single molecules can be measured in living cells. The main difficulty lies in the rapid photobleaching of conventional probes (organic dyes and fluorescent proteins) and high cellular autofluorescence. Colloidal semiconductor quantum dots are promising in this regard because they are brighter (10−20 times) and far more photostable than organic dyes. However, severe intermittence in emission (also known as blinking) has been universally observed from single dots (*60*) and has been considered an intrinsic limitation difficult to overcome. For instance, in a recent application of single quantum dot imaging, the tracking of membrane receptors was frequently interrupted due to the stroboscopic nature of recording (*61*). A surprising discovery was recently reported by Hohng and Ha (*62*) in which quantum dot blinking was all but completely suppressed by adding additives in solution, now rendering quantum dots ideal as next generation probes for single-molecule studies. This may allow continuous observation of molecular movements as long as necessary both in vitro and in vivo. Whether quantum dots can be made small enough for observing internal motion of single molecules via FRET remains to be seen.

CONCLUSION

It has become clear that single-molecule fluorescence techniques are well suited for many applications involving nucleic acids. While many technical challenges lie ahead in making these methods more powerful and general, the field is now mature enough to tackle real biological questions head on. New applications are emerging continuously, limited only by imagination.

REFERENCES

1. Weiss, S. (2000) Measuring conformational dynamics of biomolecules by single molecule fluorescence spectroscopy. *Nat. Struct. Biol. 7*, 724−729.
2. Ha, T. (2001) Single-molecule fluorescence methods for the study of nucleic acids. *Curr. Opin. in Struct. Biol. 11*, 287−292.
3. Yildiz, A., et al. (2003) Myosin V walks hand-over-hand: single fluorophore imaging with 1.5-nm localization. *Science 300*, 2061−2065.
4. Ha, T., Laurence, T. A., Chemla, D. S., and Weiss, S. (1999) Polarization spectroscopy of single fluorescent molecules. *J. Phys. Chem. B 103*, 6839−6850.
5. Jia, Y. W., et al. (1997) Nonexponential Kinetics of a Single Trna-(Phe) Molecule Under Physiological Conditions. *Proc. Natl. Acad. Sci. U.S.A. 94*, 7932−7936.
6. Lu, H. P., Iakoucheva, L. M., and Ackerman, E. J. (2001) Single-molecule conformational dynamics of fluctuating noncovalent DNA-protein interactions in DNA damage recognition. *J. Am. Chem. Soc. 123*, 9184−9185.
7. Selvin, P. R. (2000) The renaissance of fluorescence resonance energy transfer. *Nat. Struct. Biol. 7*, 730−734.
8. Jares-Erijman, E. A., and Jovin, T. M. (2003) FRET imaging. *Nat. Biotechnol. 21*, 1387−1395.
9. Ha, T. (2001) Single molecule fluorescence resonance energy transfer. *Methods 25*, 78.
10. Ha, T., et al. (1996) Probing the interaction between two single molecules − fluorescence resonance energy transfer between a single donor and a single acceptor. *Proc. Natl. Acad. Sci. U.S.A. 93*, 6264−6268.
11. Schutz, G. J., Trabesinger, W., and Schmidt, T. (1998) Direct Observation of Ligand Colocalization On Individual Receptor Molecules. *Biophys. J. 74*, 2223−2226.
12. Ha, T. J., et al. (1999) Single-molecule fluorescence spectroscopy of enzyme conformational dynamics and cleavage mechanism. *Proc. Natl. Acad. Sci. U.S.A. 96*, 893−898.
13. Deniz, A. A., et al. (1999) Single-pair fluorescence resonance energy transfer on freely diffusing molecules: Observation of Forster distance dependence and subpopulations. *Proc. Natl. Acad. Sci. U.S.A. 96*, 3670−3675.
14. Ha, T., et al. (1999) Ligand-induced conformational changes observed in single RNA molecules. *Proc. Natl. Acad. Sci. U.S.A. 96*, 9077−9082.
15. Zhuang, X. W., et al. (2000) A single-molecule study of RNA catalysis and folding. *Science 288*, 2048−2051.
16. Ha, T., et al. (2000) Initiation and reinitiation of DNA unwinding by the *Escherichia coli* Rep helicase. *Nature 419*, 638−641.
17. McKinney, S. A., Declais, A. C., Lilley, D. M. J., and Ha, T. (2003) Structural dynamics of individual Holliday junctions. *Nat. Struct. Biol. 10*, 93−97.

18. Tan, E., et al. (2003) A four way junction accelerates hairpin ribozyme folding via a discrete intermediate. *Proc. Natl. Acad. Sci. U.S.A. 100*, 9308.
19. Talaga, D. S., et al. (2000) Dynamics and folding of single two-stranded coiled-coil peptides studied by fluorescent energy transfer confocal microscopy. *Proc. Natl. Acad. Sci. U.S.A. 97*, 13021−13026.
20. Schuler, B., Lipman, E. A., and Eaton, W. A. (2002) Probing the free-energy surface for protein folding with single-molecule fluorescence spectroscopy. *Nature 419*, 743−747.
21. Deniz, A. A., et al. (2000) Single-molecule protein folding: Diffusion fluorescence resonance energy transfer studies of the denaturation of chymotrypsin inhibitor 2. *Proc. Natl. Acad. Sci. U.S.A. 97*, 5179−5184.
22. Bokinsky, G., et al. (2003) Single-molecule transition-state analysis of RNA folding. *Proc. Natl. Acad. Sci. U.S.A. 100*, 9302−9307.
23. Bartley, L. E., Zhuang, X., Das, R., Chu, S., and Herschlag, D. (2003) Exploration of the transition state for tertiary structure formation between an RNA helix and a large structured RNA. *J. Mol. Biol. 328*, 1011−1026.
24. Ying, L., Green, J. J., Li, H., Klenerman, D., and Balasubramanian, S. (2003) Studies on the structure and dynamics of the human telomeric G quadruplex by single-molecule fluorescence resonance energy transfer. *Proc. Natl. Acad. Sci. U.S.A. 100*, 14629−14634.
25. Hohng, S., et al. (2004) Conformational flexibility of four-way junctions in RNA. *J. Mol. Biol. 336*, 69−79.
26. Rothwell, P. J., et al. (2003) Multiparameter single-molecule fluorescence spectroscopy reveals heterogeneity of HIV-1 reverse transcriptase: primer/template complexes. *Proc. Natl. Acad. Sci. U.S.A. 100*, 1655−1660.
27. Borsch, M., Diez, M., Zimmermann, B., Reuter, R., and Graber, P. (2002) Stepwise rotation of the gamma-subunit of EF(0)F(1)-ATP synthase observed by intramolecular single-molecule fluorescence resonance energy transfer. *FEBS Lett. 527*, 147−152.
28. Russell, R., et al. (2002) Exploring the folding landscape of a structured RNA. *Proc. Natl. Acad. Sci. U.S.A. 99*, 155−160.
29. Sako, Y., Minoghchi, S., and Yanagida, T. (2000) Single-molecule imaging of EGFR signalling on the surface of living cells. *Nat. Cell Biol. 2*, 168−172.
30. Yasuda, R., et al. (2003) The ATP-waiting conformation of rotating F1-ATPase revealed by single-pair fluorescence resonance energy transfer. *Proc. Natl. Acad. Sci. U.S.A. 100*, 9314−9318.
31. Kim, H. D., et al. (2002) Mg^{2+}-dependent conformational change of RNA studied by fluorescence correlation and FRET on immobilized single molecules. *Proc. Natl. Acad. Sci. U.S.A. 99*, 4284−4289.
32. Chen, Y., Hu, D., Vorpagel, E. R., and Lu, H. P. (2003) Probing Single-Molecule T4 Lysozyme Conformational Dynamics by Intramolecular Fluorescence Energy Transfer. *J. Phys. Chem. B 107*, 7947−7956.
33. Rasnik, I., Myong, S., Cheng, W., Lohman, T. M., and Ha, T. (2004) DNA-binding orientation and domain conformation of the E. coli Rep helicase monomer bound to a partial duplex junction: Single-molecule studies of fluorescently labeled enzymes. *J. Mol. Biol. 336*, 395−498.
34. Braslavsky, I., Hebert, B., Kartalov, E., and Quake, S. R. Sequence information can be obtained from single DNA molecules. *Proc. Natl. Acad. Sci. U.S.A. 100*, 3960−3964.
35. Deniz, A. A., et al. (2001) Ratiometric single-molecule studies of freely diffusing biomolecules. *Annu. Rev. Phys. Chem. 52*, 233−253.
36. Zhuang, X. W., et al. (2002) Correlating structural dynamics and function in single ribozyme molecules. *Science 296*, 1473−1476.
37. Lu, H. P., Xun, L. Y., and Xie, X. S. (1998) Single-molecule enzymatic dynamics. *Science 282*, 1877−1882.
38. Lilley, D. M. J., and White, M. F. (2001) The junction-resolving enzymes. *Nat. Rev. Mol. Cell Biol. 2*, 433−443.
39. Clegg, R. M., Murchie, A. I. H., and Lilley, D. M. J. (1994) The Solution Structure of the Four-Way DNA Junction At Low-Salt Conditions − a Fluorescence Resonance Energy Transfer Analysis. *Biophys. J. 66*, 99−109.
40. Duckett, D. R., et al. (1988) The structure of the Holliday junction, and its resolution. *Cell 55*, 79−89.
41. Murchie, A. I., et al. (1989) Fluorescence energy transfer shows that the four-way DNA junction is a right-handed cross of antiparallel molecules. *Nature 341*, 763−766.
42. Miick, S. M., Fee, R. S., Millar, D. P., and Chazin, W. J. (1997) Crossover Isomer Bias Is the Primary Sequence-Dependent Property of Immobilized Holliday Junctions. *Proc. Natl. Acad. Sci. U.S.A. 94*, 9080−9084.
43. Grainger, R. J., Murchie, A. I. H., and Lilley, D. M. J. (1998) Exchange Between Stacking Conformers in a Four-Way DNA Junction. *Biochemistry 37*, 23−32.
44. Eichman, B. F., Vargason, J. M., Mooers, B. H. M., and Ho, P. S. (2000) The Holliday junction in an inverted repeat DNA sequence: Sequence effects on the structure of four-way junctions. *Proc. Natl. Acad. Sci. U.S.A. 97*, 3971−3976.
45. Panyutin, I. G., and Hsieh, P. (1994) The Kinetics of Spontaneous DNA Branch Migration. *Proc. Natl. Acad. Sci. U.S.A. 91*, 2021−2025.
46. Wang, Y., and Patel, D. J. (1993) Solution structure of the human telomeric repeat d[AG3(T2AG3)3] G-tetraplex. *Structure 1*, 263−282.
47. Parkinson, G. N., Lee, M. P., and Neidle, S. (2002) Crystal structure of parallel quadruplexes from human telomeric DNA. *Nature 417*, 876−880.
48. Ren, X., et al. (2003) Identification of a new RNA. RNA interaction site for human telomerase RNA (hTR): structural implications for hTR accumulation and a dyskeratosis congenita point mutation. *Nucleic Acids Res. 31*, 6509−6515.
49. Katiliene, Z., Katilius, E., and Woodbury, N. W. (2003) Single Molecule Detection of DNA Looping by NgoMIV Restriction Endonuclease. *Biophys. J. 84*, 4053−4061.
50. Lohman, T. M., and Bjornson, K. P. (1996) Mechanisms of helicase-catalyzed DNA unwinding. *Annu. Rev. Biochem. 65*, 169−214.
51. Bianco, P. R., et al. (2001) Processive translocation and DNA unwinding by individual RecBCD enzyme molecules. *Nature 409*, 374−378.
52. Dohoney, K. M., and Gelles, J. (2001) Chi-Sequence recognition and DNA translocation by single RecBCD helicase/nuclease molecules. *Nature 409*, 370−374.
53. Cheng, W., Hsieh, J., Brendza, K. M., and Lohman, T. M. (2001) *E. coli* Rep Oligomers Are Required to Initiate DNA Unwinding In Vitro. *J. Mol. Biol. 310*, 327−350.
54. Ishijima, A., et al. (1998) Simultaneous Observation of Individual ATPase and Mechanical Events By a Single Myosin Molecule During Interaction With Actin. *Cell 92*, 161−171.
55. Harada, Y., et al. (1999) Single-molecule imaging of RNA polymerase-DNA interactions in real time. *Biophys. J. 76*, 709−715.
56. Borisenko, V., et al. (2003) Simultaneous optical and electrical recording of single gramicidin channels. *Biophys. J. 84*, 612−622.
57. Harms, G. S., et al. (2003) Probing conformational changes of gramicidin ion channels by single-molecule patch-clamp fluorescence microscopy. *Biophys. J. 85*, 1826−1838.
58. Lang, M. J., Fordyce, P. M., and Block, S. M. (2003) Combined optical trapping and single-molecule fluorescence. *J. Biol. 2*, 6.
59. Liphardt, J., Onoa, B., Smith, S. B., Tinoco, I., and Bustamante, C. (2001) Reversible unfolding of single RNA molecules by mechanical force. *Science 292*, 733−737.
60. Nirmal, M., et al. (1996) Fluorescence Intermittency in Single Cadmium Selenide Nanocrystals. *Nature 383*, 802−804.
61. Dahan, M., et al. (2003) Diffusion dynamics of glycine receptors revealed by single-quantum dot tracking. *Science 302*, 442−445.
62. Hohng, S., and Ha, T. (2004) Near complete suppression of quantum dot blinking in ambient conditions. *J. Am. Chem. Soc. 126*, 1324−1325.

BI049973S